Ferromagnetism in structurally disordered UFe0.39Ge2

Maria Szlawska, Mathieu Pasturel, Dariusz Kaczorowski, Adam Pikul

▶ **To cite this version:**

Maria Szlawska, Mathieu Pasturel, Dariusz Kaczorowski, Adam Pikul. Ferromagnetism in structurally disordered UFe0.39Ge2. Journal of Alloys and Compounds, 2022, 892, pp.162032. 10.1016/j.jallcom.2021.162032 . hal-03414042

HAL Id: hal-03414042
https://hal.science/hal-03414042v1

Submitted on 30 May 2022

HAL is a multi-disciplinary open access archive for the deposit and dissemination of scientific research documents, whether they are published or not. The documents may come from teaching and research institutions in France or abroad, or from public or private research centers.

L'archive ouverte pluridisciplinaire **HAL**, est destinée au dépôt et à la diffusion de documents scientifiques de niveau recherche, publiés ou non, émanant des établissements d'enseignement et de recherche français ou étrangers, des laboratoires publics ou privés.

Distributed under a Creative Commons Attribution - NonCommercial - NoDerivatives 4.0 International License

Journal of Alloys and Compounds 892 (2021) 162032

Contents lists available at ScienceDirect

Journal of Alloys and Compounds

journal homepage: www.elsevier.com/locate/jalcom

Ferromagnetism in structurally disordered $UFe_{0.39}Ge_2$

Maria Szlawska[a,*], Mathieu Pasturel[b], Dariusz Kaczorowski[a], Adam Pikul[a]

[a] Institute of Low Temperature and Structure Research, Polish Academy of Sciences, Wrocław, Poland
[b] Université de Rennes 1, Institut des Sciences Chimiques de Rennes, UMR CNRS 6226, Rennes, France

ARTICLE INFO

Article history:
Received 10 June 2021
Received in revised form 6 September 2021
Accepted 16 September 2021
Available online 23 September 2021

Keywords:
Uranium intermetallics
Uranium germanides
Crystal structure
Bulk physical properties
Cluster glass
Disorder effects

ABSTRACT

A polycrystalline sample of the uranium ternary germanide $UFe_{0.39}Ge_2$ was examined by means of X-ray powder diffraction, DC magnetization and AC magnetic susceptibility, heat capacity and electrical resistivity measurements performed in wide ranges of temperature and magnetic fields. The experiments confirmed that the compound crystallizes with orthorhombic crystal structure of the $CeNiSi_2$-type that is closely related to that of the ferromagnetic superconductor UGe_2 and orders ferromagnetically at 37 K. Moreover, it exhibits some features characteristic of ferromagnetic cluster glasses. The electrical transport in $UFe_{0.39}Ge_2$ is strongly influenced by structural disorder arising from the partly occupied Fe-sites in its crystallographic unit cell.

© 2021 The Author(s). Published by Elsevier B.V.
CC_BY_NC_ND_4.0

1. Introduction

Uranium-based intermetallic phases often exhibit unique physical properties that result in most cases from interactions of electrons from conduction band with those from partly occupied 5*f* shells of periodically arranged uranium ions. In that context, uranium germanides have attracted special attention, ignited by a seminal discovery in 2000 of unconventional superconductivity in the ferromagnetically ordered compound UGe_2 [1] that crystallizes with an orthorhombic unit cell of the $ZrGa_2$ type (space group *Cmmm*) [2,3]. This finding has been followed by an intense search for other materials harboring the coexistence of ferromagnetism and superconductivity that are commonly considered as antagonistic physical phenomena. As a result, two ternary germanides have been identified as superconducting ferromagnets, namely URhGe [4] and UCoGe [5], both crystallizing with the orthorhombic TiNiSi-type unit cell (space group *Pnma*) [6,7]. Interestingly, a common feature of the crystal structures of those ternaries and that of UGe_2 is the presence of zig-zag chains of the U atoms with the U-U distances close to the Hill limit for uranium compounds (i.e. 3.5 Å) [8].

Recently, we begun systematic re-investigation of another family of ternary uranium germanides, namely $UTE_{1-x}Ge_2$, where *TE* stands for a transition-metal element. Our research revealed the formation of two novel ferromagnets, $URu_{0.29}Ge_2$ (T_C = 63 K) [9] and $UOs_{0.25}Ge_2$ (T_C = 54 K, unpublished), crystallizing with a new type of monoclinic structure (space group $C2/c$). Moreover, we confirmed the existence of antiferromagnetic $UNi_{0.45}Ge_2$ (T_N = 47 K) [10] that crystallizes with the orthorhombic $CeNiSi_2$-type unit cell (space group *Cmcm*). It is worth noting, that the monoclinic $URu_{0.29}Ge_2$-type structure and the orthorhombic $CeNiSi_2$-type structure can be considered as close derivatives of the orthorhombic $ZrGa_2$ type structure adopted by UGe_2. In turn, an important distinction between those three structures is significantly different distances between the U-atom chains [9,10].

The compound $UFe_{1-x}Ge_2$ is another representative of the $UTE_{1-x}Ge_2$ family, reported by Henriques *et al.* to form with an extended homogeneity range $0.58 < 1-x < 0.78$, [11]. It crystallizes with a *TE*-deficient orthorhombic structure of the $CeNiSi_2$ type, alike $UNi_{0.45}Ge_2$. In this paper, we report the results of our study of the physical properties of $UFe_{0.39}Ge_2$, performed in wide ranges of temperature and magnetic field.

2. Experimental details

Several polycrystalline samples of $UFe_{1-x}Ge_2$ ($0.55 \leqslant x \leqslant 0.80$) were obtained by arc-melting (Bühler MAM1 furnace) the corresponding amounts of the elemental components (purity of each > 99.5 at%) in purified argon atmosphere. To ensure homogeneity of the products, the buttons were turned over and remelted several times. Subsequently, they were enclosed in an evacuated quartz tube and annealed at 900 K for four weeks.

* Corresponding author.
E-mail address: m.szlawska@intibs.pl (M. Szlawska).

https://doi.org/10.1016/j.jallcom.2021.162032
0925-8388/© 2021 The Author(s). Published by Elsevier B.V.
CC_BY_NC_ND_4.0

Quality of the samples was checked using powder X-ray diffraction (XRD) in reflection mode on a Bruker D8 Advance diffractometer operating with monochromatized Cu Kα1 radiation (λ = 1.5406 Å), equipped with a LynxEye fast detector to select X-ray energy and thus remove the Fe-fluorescence signal. The diffraction patterns were analyzed by the Rietveld method using the Fullprof Suite software [12]. The composition of the samples was verified using energy dispersive spectroscopy (SDD X-Max 50 mm^2 Oxford Instruments EDS) on a scanning electron microscope (JEOL JSM 7100F SEM).

DC magnetic measurements were performed on a selected sample in the form of bulk piece (see below) in the temperature range 1.72–400 K and in magnetic fields up to 70 kOe. AC magnetic susceptibility was measured at 32–40 K in zero external DC magnetic field using an alternate probing magnetic field with an amplitude of 3.7 Oe and a frequency from 1 Hz to 1 kHz. Both experiments were carried out using a Quantum Design MPMS-7 SQUID (superconducting quantum interference device) magnetometer. Heat capacity was measured from 2 to 300 K and in magnetic fields up to 10 kOe using a thermal relaxation technique. Electrical resistivity of a bar-shaped sample was measured in the temperature range 2–300 K and in magnetic fields up to 90 kOe using a conventional four-probe AC method in the field cooling regime and upon decreasing the temperature. The heat capacity and electrical transport experiments were carried out employing a Quantum Design PPMS-9 platform.

3. Results and discussion

3.1. Chemical composition and crystal structure

Due to a non-congruent character of the formation of $UFe_{1-x}Ge_2$ and a large number of phases being in equilibrium in the ternary phase diagram U-Fe-Ge [11], several samples with different compositions were synthesized along the solid-solution line $UFe_{1-x}Ge_2$. It allowed to control the formation of secondary phases that was generally aimed at decreasing their amount as much as possible. In particular, we successfully avoided the contamination of the main phase by ferromagnetic UGe_2 (T_C = 52 K [13]), U_3Ge_5 (T_C = 94 K [14]), $U_3Fe_4Ge_4$ (T_C = 17 K [15]) and $U_{34}Fe_4Ge_{33}$ (T_C = 28 K [16]). In turn, in each sample we found some amount of the ferromagnetically ordered impurity $U_3Fe_2Ge_7$ (T_C = 62 K [17]). In our attempts, we allowed for the presence of paramagnetic phases, like e.g. UGe_3 [18], $U_9Fe_7Ge_{24}$ [19] or UFe_2Ge_2 [20,21], expecting them to be less deleterious to investigate the physical properties of the desired phase $UFe_{1-x}Ge_2$.

As the final result of all these efforts, we selected for the physical properties measurements a sample with the initial composition 1U-0.45Ge-2Ge, which (besides the major phase) contained only two additional phases in small amounts. The SEM-EDS analysis (see the inset to Fig. 1) revealed that the majority phase in this specimen forms large and homogeneous grains with an average composition 29.89U-11.54Fe-58.57Ge (in at%) that corresponds to $UFe_{0.39(2)}Ge_2$. This Fe-atom content is slightly lower than the lower limit ($1-x$ = 0.42) derived by Henriques *et al.* for the solid solution $UFe_{1-x}Ge_2$ at 1173 K [11]. The two secondary phases were found exclusively at grain boundaries and had the compositions: 26.02U-15.77Fe-58.21Ge, which corresponds to $U_3Fe_2Ge_7$, and 22.91U-22.21Fe-54.88Ge. The latter phase significantly deviates from any other known ternary alloy in the system U-Fe-Ge and might be a novel ternary compound. Alternatively, it can be attributed to a Fe/Ge solubility domain in $U_9Fe_7Ge_{24}$ (note that 22.5U-17.5Fe-60.0Ge is expected for $U_9Fe_7Ge_{27}$).

Based on those findings, the powder XRD pattern (Fig. 1) was easily indexed with the orthorhombic unit cells of $UFe_{1-x}Ge_2$ and $U_3Fe_2Ge_7$. The remaining small extra diffraction peaks seen in the pattern were found to appear at 2θ values near the Bragg peaks positions generated for $U_9Fe_7Ge_{24}$, yet with significant deviation from the expected intensities. Nevertheless, the Rietveld refinement was performed considering these three phases and the results are shown in Fig. 1 and summarized in Tab. 1. In particular, $UFe_{1-x}Ge_2$ has been confirmed to adopt the transition-metal-deficient orthorhombic $CeNiSi_2$-type structure [11] with the cell parameters a = 4.0886(1) Å, b = 15.8339(3) Å and c = 4.0505(1) Å. It should be noted that the absence of splitting of the main Bragg peak (131) rules out the monoclinic distortion observed in $URu_{0.29}Ge_2$ [9]. The refined atomic coordinates agree with the structural model proposed by Henriques et al. [11], and the derived occupancy of the Fe-atom site leads to a chemical formula $UFe_{0.32(1)}Ge_2$, slightly poorer in iron than that obtained from the EDS experiments. The refinements showed that the content of the two impurities were 2(1) wt% of $U_3Fe_2Ge_7$ and about 3(1) wt% of "$U_9Fe_7Ge_{24}$".

3.2. Magnetic properties

Fig. 2 (a) shows the temperature dependence of the inverse molar magnetization divided by the magnetic field, $(M/H)^{-1}(T)$, of $UFe_{0.39}Ge_2$. Above about 130 K, it exhibits slightly curvilinear behavior, which can be described by the modified Curie-Weiss law $M/H(T) = \chi_0 + (\mu_{eff}^2/8)/(T-\theta_P)$, where μ_{eff} denotes the effective magnetic moment and θ_P stands for the paramagnetic Curie-Weiss temperature. Least-square fitting of that formula to the experimental data yielded μ_{eff} = 2.59 μ_B, θ_P = 30 K, and $\chi_0 = 1\times10^{-4}$ emu mol^{-1}. The so-obtained μ_{eff} is much smaller than the values predicted for free U^{3+} and U^{4+} ions (3.62 and 3.58 μ_B, respectively), but it is large enough to ascribe the observed magnetic properties of the compound exclusively to the uranium ions. The discrepancy can be attributed to partial delocalization of 5f electrons, magnetocrystalline anisotropy and/or crystal field effect. The positive sign of θ_P hints at predominance of ferromagnetic exchange interactions.

Below about 37 K, the $M(T)$ variation of $UFe_{0.39}Ge_2$ displays an anomaly with a Brillouin-like curvature (see the upper inset to Fig. 2(a)) that manifests a ferromagnetic phase transition. Pronounced difference between the magnetization curves measured in zero-field-cooled (ZFC) and field-cooled (FC) regimes results from formation and reorientation of ferromagnetic domains. Also the magnetization isotherm $M(H)$ measured at 1.7 K, the lowest temperature available in the experiment, is typical for long-range ferromagnetic ordering (see the lower inset to Fig. 2(a)). At 70 kOe, $M(H)$ achieves a value of about 9.9 emu g^{-1}, which corresponds to the magnetic moment of 0.72 μ_B per formula unit, being a reasonable value for uranium intermetallics.

As can be seen in Fig. 2(b), the difference between the $M(T)$ curves in the ordered region systematically diminishes with increasing magnetic field, and in 10 kOe it is visible only at the lowest temperature studied. At the same time, the anomaly associated with the magnetic ordering smears out and moves towards higher temperature. Both behaviors are characteristic of ferromagnets.

The temperature variation of the AC magnetic susceptibility χ_{AC} of $UFe_{0.39}Ge_2$ is plotted in Fig. 3. The real and imaginary components of the susceptibility (χ' and χ'', respectively) show distinct maxima at T_{max}, which can be associated with the magnetic ordering at T_C = 37 K.

The value of T_{max} in $\chi'(T)$ equals 36.1 K for the probing AC magnetic field frequency f_{AC} = 1 Hz. With increasing f_{AC}, T_{max} increases up to 36.3 K in f_{AC} = 1 kHz. Such a behavior of $\chi'(T)$ is often considered as a fingerprint of spin-glass-like ground state [22]. For spin glasses, one can identify T_{max} as a freezing temperature T_f, and calculate its relative shift upon change of f_{AC}, $\delta T_f = \frac{\Delta T_f}{T_f \Delta \log f_{AC}}$. For typical non-magnetic metallic spin glasses with strong structural disorder, this parameter is of the order of 10^{-2} (e.g., δT_f = 0.036 in

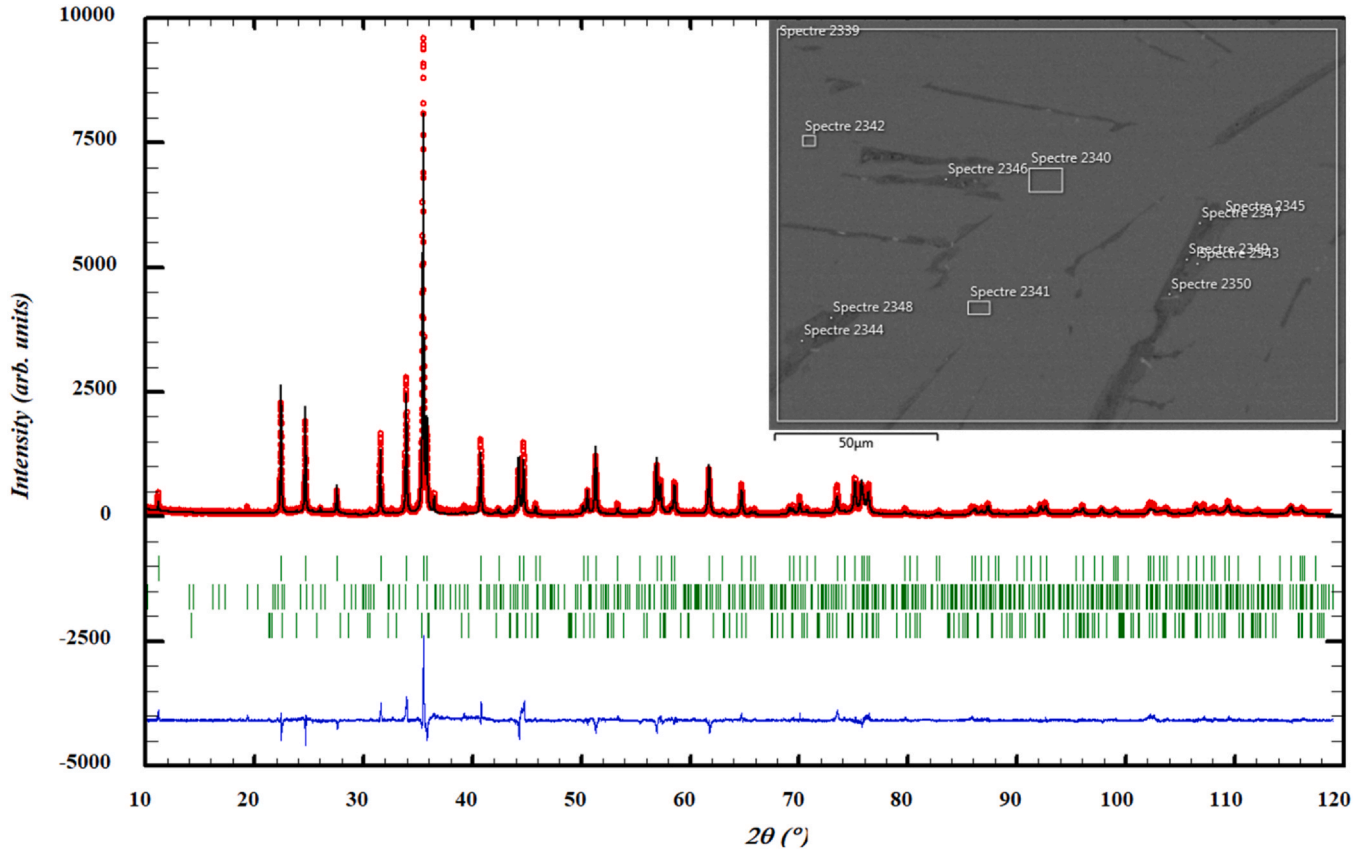

Fig. 1. Rietveld-refined powder XRD pattern of the sample "$UFe_{0.45}Ge_2$". Red circles display the experimental data, black line represents the theoretical pattern, and blue curve shows the difference between them. Vertical ticks mark the Bragg positions calculated for $UFe_{1-x}Ge_2$, $U_9Fe_7Ge_{24}$ and $U_3Fe_2Ge_7$ (top, middle and bottom ticks, respectively). The inset shows a backscattered electron SEM image of the sample studied with the examined areas marked; a majority phase ($UFe_{0.39(2)}Ge_2$) is visible as dominating gray area, while the two secondary phases (i.e. $U_3Fe_2Ge_7$ and a phase with the composition 22.91U-22.21Fe-54.88Ge, in at%) are represented as dark gray inclusions. (For interpretation of the references to color in this figure legend, the reader is referred to the web version of this article.).

Table 1
Crystal structure data of "$UFe_{0.45}Ge_2$" obtained by Rietveld analysis of the powder XRD pattern.

Formula	$UFe_{1-x}Ge_2$						
Structure type	$CeNiSi_2$						
Space group	*Cmcm* (no. 63)						
Cell parameters (Å)	a = 4.0886(1); b = 15.8339(3); c = 4.0505(1)						
Atomic positions	Atom	Wyckoff	x	y	z	Occ.	B_{iso} (Å^2)
	U1	4*c*	0	0.3966(1)	1/4	1	0.83(2)
	Fe1	4*c*	0	0.1978(9)	1/4	0.32(2)	2.3(4)
	Ge1	4*c*	0	0.0681(3)	1/4	1	4.5(2)
	Ge2	4*c*	0	0.7495(2)	1/4	1	0.69(7)
Reflections/ refined parameters	146/24						
Reliability factors	χ^2 = 4.75						
	R_p = 25.2; R_{wp} = 27.8; R_{exp} = 12.78						
	R_{Bragg} = 12.1; R_F = 6.49						

Pr_2NiSi_3 [23], and δT_f = 0.025 in or URh_2Ge_2 [24]). The value of δT_f estimated for $UFe_{0.39}Ge_2$ is as small as 0.002, i.e. one order of magnitude lower than expected for spin glasses. Nevertheless, it is worth noting that it is similar to those reported for ferromagnetic cluster glasses with large spin clusters, such as Pr_2CuSi_3 (δT_f = 0.001) and Nd_2CuSi_3 (δT_f = 0.002) [25].

3.3. Heat capacity

Fig. 4 (a) shows temperature dependence of the specific heat C_P of $UFe_{0.39}Ge_2$ measured in zero magnetic field. As seen, at room temperature C_P attains a value of about 88 J K^{-1} mol^{-1}, which is close to the Dulong-Petit limit $3nR$ (where n is a number of atoms per molecule and R is the universal gas constant) calculated for the compound studied (n = 3.39), i.e. 85 J K^{-1} mol^{-1}. The ferromagnetic phase transition at T_C = 37 K manifests itself in the $C_P(T)$ curve as a λ-shaped anomaly. However, the peak in the heat capacity data is rather broad and its shape is similar to that reported for the cluster-glass systems U_2RhSi_3 [26], U_2IrSi_3 [27,28], and U_2CoSi_3 [29].

The inset to Fig. 4(a) displays C_P/T of $UFe_{0.39}Ge_2$ plotted as a function of T^2. Below about 6 K, the experimental curve exhibits nearly linear behavior, which can be described as a sum $C_P(T) = \gamma T + \beta T^3$, where the first term represents the Sommerfeld contribution, while the second term accounts for the phonon contribution approximated by the Debye law. The numerical analysis yielded γ = 123(1) mJ K^{2}mol^{-1} and $\beta = 3.9(2)\times10^{-4}$ mJ K^{4}mol^{-1}. Using the formula

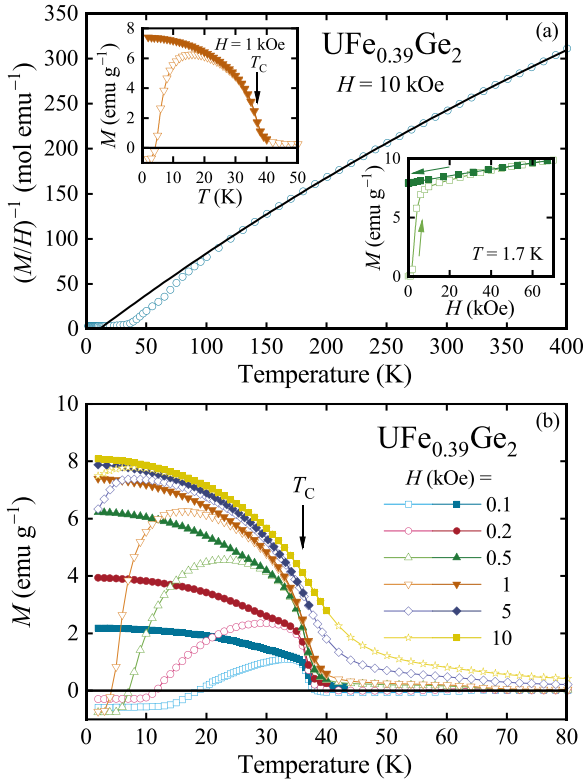

Fig. 2. (a) Temperature dependence of inverse molar magnetization divided by the magnetic field $(M/H)^{-1}$ of $UFe_{0.39}Ge_2$; solid line is a fit of the modified Curie-Weiss law to the experimental data (for details see the text). Upper inset: low-temperature variation of magnetization M measured in zero-field-cooling (closed symbols) and field-cooling (open symbols) regimes; an arrow marks temperature of magnetic ordering T_C. Lower inset: M measured at the lowest temperature available as a function of increasing (open symbols) and decreasing (closed symbols) external magnetic field H. (b) $M(T)$ studied in various magnetic fields.

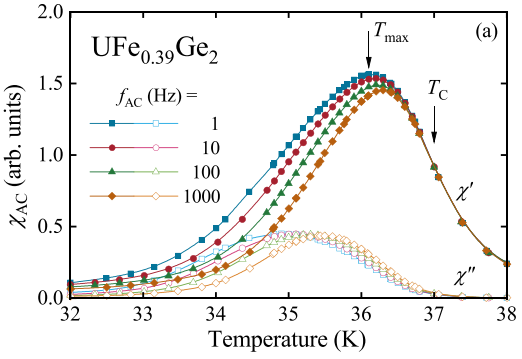

Fig. 3. Dynamic magnetic susceptibility χ_{AC} of $UFe_{0.39}Ge_2$ measured as a function of temperature with various frequencies f; χ' and χ'' stand for the real and imaginary part of the susceptibility, respectively.

$\Theta_D = \sqrt[3]{1944n/\beta}$, one finds the Debye temperature Θ_D = 257(5) K that is of the order of magnitude characteristic of intermetallic compounds.

Remarkably, the Sommerfeld coefficient derived for $UFe_{0.39}Ge_2$ has a significantly higher value than usually observed in U-bearing systems. Similar enhancement of the γ coefficient in uranium intermetallics is often considered as originating from the presence of strong electronic correlations. However, an enlarged linear contribution to the low-temperature specific heat is also a characteristic feature of structurally disordered systems [22]. The excess of specific heat results from the magnetic entropy surviving to low temperatures due to frustrated and degenerate nature of the ground state. In

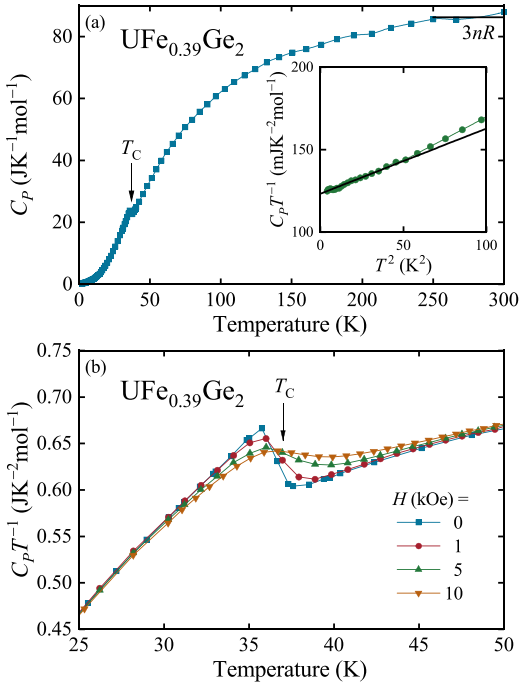

Fig. 4. (a) Temperature variation of specific heat C_P of $UFe_{0.39}Ge_2$; an arrow marks the ordering temperature T_C and the horizontal line points at the Dulong-Petit limit calculated for the compound. Inset: low temperature C_P/T-ratio as a function of T^2; solid line is a fit of a sum of the Debye-T^3 law and the Sommerfeld coefficient to the experimental data (for details see the text). (b) C_PT^{-1} vs. T measured in magnetic field.

some special cases such enhancement in C/T could be a false indicator of heavy-fermion behavior [30].

In this context, it is worth recalling that the γ value reported for the crystallographically ordered ferromagnet UGe_2 equals 33 mJ K^{-2}mol^{-1} (see Ref. [31] and references therein), while that derived for the closely related ferromagnetic compound $URu_{0.29}Ge_2$ with partly occupied Ru-sites is twice larger (61 mJ K^{-2}mol^{-1} [9]). By analogy, given the inherent crystallographic disorder in $UFe_{0.39}Ge_2$, the obtained large value of γ seems to originate from its structural features, and rather unlikely from strong electronic correlations.

As can be seen in Fig. 4(b), upon applying the magnetic field, the anomaly in $C_P(T)$ associated with the magnetic phase transition at T_C significantly broadens and moves towards higher temperature, which confirms the ferromagnetic-like character of the ordering. Similar behavior was observed in ferromagnetic $URu_{0.29}Ge_2$ [9].

3.4. Electrical resistivity

Fig. 5 (a) displays the temperature dependence of the electrical resistivity of $UFe_{0.39}Ge_2$. Overall, the magnitude of ρ is rather large and hardly varies with changing temperature. Both features are typical for metals with strong crystallographic disorder.

Near 190 K, the $\rho(T)$ curve forms a broad maximum characteristic of semimetallic systems. At T_C = 37 K, $\rho(T)$ exhibits a sharp dip, followed by rapid upturn in the ordered state. The latter behavior hints at more complex spin arrangement in $UFe_{0.39}Ge_2$ than a simple collinear ferromagnetism. Interestingly, a very similar deep minimum at the respective T_C was observed before for U_2CoSi_3 [29] and U_2IrSi_3 [27,28], where it was identified as a signature of cluster glass state in metallic systems with disordered crystal structures. It seems likely that the electronic transport behavior in $UFe_{0.45}Ge_2$ can also be attributed to the emergence at low temperature of ferromagnetic cluster-glass regime.

Most remarkably, the upturn in $\rho(T)$ can be entirely suppressed by as small magnetic field as 1 kOe (see Fig. 5(b)). The resistivity

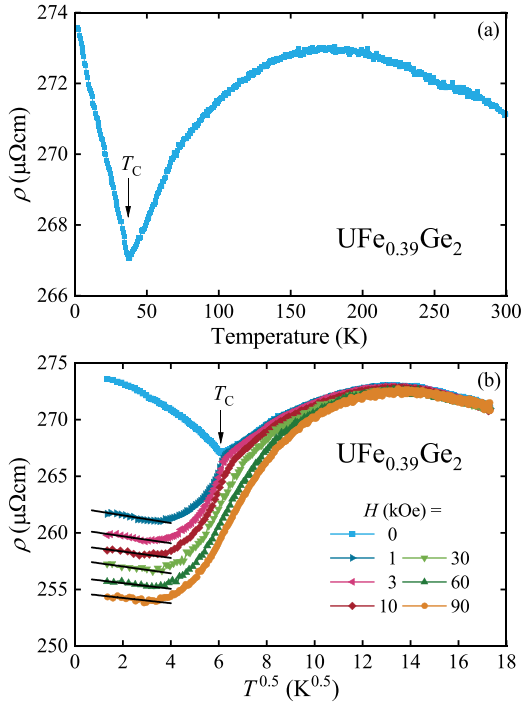

Fig. 5. (a) Electrical resistivity ρ of $UFe_{0.39}Ge_2$ as a function of temperature. (b) ρ vs. $T^{0.5}$ measured in various magnetic fields; solid lines show $\rho(T) \propto -T^{0.5}$ dependence at low temperature.

measured in applied field varies with temperature in a manner expected for ferromagnets, i.e. $\rho(T)$ shows a kink at T_C, and its position shifts towards higher temperatures with increasing the field strength. Also the magnitude of the resistivity diminishes with increasing field, signaling gradual suppression of ferromagnetic fluctuations.

Below about 16 K, the resistivity measured in finite external magnetic field increases with decreasing temperature. As can be inferred from Fig. 5(b), $\rho(T)$ has there a $-T^{0.5}$ slope that is independent of the strength of magnetic field at least up to 90 kOe. The relative change of the resistivity in this temperature range is only +0.3%. Such a small and field-independent change of the resistivity with the $-T^{0.5}$ variation points at possible presence of quantum interference effects, such as electron-electron interactions or weak localization. Quantum correction to $\rho(T)$ of $UFe_{0.39}Ge_2$ can be expected to occur because of distinct crystallographic disorder in its unit cell, and would manifest itself in a similar manner as reported for several disordered U-based intermetallics, such as U_2CoSi_3 [29] or U_2NiSi_3 [32].

4. Summary

Our studies confirmed that $UFe_{0.39}Ge_2$ crystallizes with the Ni-deficient orthorhombic $CeNiSi_2$-type structure and orders ferromagnetically at T_C = 37 K. The phase transition manifests itself as pronounced anomalies in the temperature variations of magnetization, AC magnetic susceptibility, specific heat and electrical resistivity of the compound, and the evolution of that phase transition in external magnetic field is in accord with its ferromagnetic character. The vacancies on the Fe-sites are a source of significant crystallographic disorder that leads to some additional features in the temperature characteristics studied, *i.a.* some frequency dependence of the dynamic susceptibility, enlarged electronic contribution to the specific heat, large magnitude of the resistivity and its small, field-independent increase at the lowest temperatures. Another possible explanation of the anomalous behavior of the thermodynamic and transport properties of $UFe_{0.39}Ge_2$ near T_C could be the formation of ferromagnetic cluster-glass state, but this conjecture needs to be verified by further experimental studies.

CRediT authorship contribution statement

Maria Szlawska: Investigation, Formal analysis, Writing – original draft. **Mathieu Pasturel:** Investigation, Formal analysis, Writing – original draft. **Dariusz Kaczorowski:** Formal analysis, Writing – review & editing. **Adam Pikul:** Formal analysis, Writing – review & editing.

Declaration of Competing Interest

The authors declare that they have no known competing financial interests or personal relationships that could have appeared to influence the work reported in this paper.

Acknowledgements

The project is co-financed by the Polish National Agency for Academic Exchange NAWA and Campus France within the PHC Polonium program (project no. PPN/BFR/2020/1/00022/U/00001).

References

[1] S. Saxena, P. Agarwal, K. Ahilan, F. Grosche, R. Haselwimmer, M. Steiner, E. Pugh, I. Walker, S. Julian, P. Monthoux, G. Lonzarich, A. Huxley, I. Sheikin, D. Braithwaite, J. Flouquet, Superconductivity on the border of itinerant-electron ferromagnetism in UGe_2, Nature 406 (2000) 587, https://doi.org/10.1038/35020500
[2] K. Oikawa, T. Kamiyama, H. Asano, Y. Ōnuki, M. Kohgi, Crystal structure of UGe_2, J. Phys. Soc. Jpn. 65 (1996) 3229, https://doi.org/10.1143/JPSJ.65.3229
[3] P. Boulet, A. Daoudi, M. Potel, H. Noël, G.M. Gross, G. André, F. Bourée, Crystal and magnetic structure of the binary uranium digermanide UGe_2, J. Alloys Compd. 247 (1997) 104, https://doi.org/10.1016/S0925-8388(96)02600-X
[4] D. Aoki, A. Huxley, E. Ressouche, D. Braithwaite, J. Flouquet, J.-P. Brison, E. Lhotel, C. Paulsen, Coexistence of superconductivity and ferromagnetism in URhGe, Nature 413 (2001) 613, https://doi.org/10.1038/35098048
[5] N.T. Huy, A. Gasparini, D.E. de Nijs, Y. Huang, J.C.P. Klaasse, T. Gortenmulder, A. de Visser, A. Hamann, T. Görlach, H. v. Löhneysen, Superconductivity on the border of weak itinerant ferromagnetism in UCoGe, Phys. Rev. Lett. 99 (2007) 067006, https://doi.org/10.1103/PhysRevLett.99.067006
[6] V. Tran, R. Troć, G. André, Magnetic ordering in URhSi and URhGe, J. Magn. Magn. Mater. 186 (1998) 81, https://doi.org/10.1016/S0304-8853(98)00074-2
[7] F. Canepa, P. Manfrinetti, M. Pani, A. Palenzona, Structural and transport properties of some UTX compounds where T=Fe, Co, Ni and X=Si, Ge, J. Alloys Compd. 234 (1996) 225, https://doi.org/10.1016/0925-8388(95)02037-3
[8] D. Aoki, K. Ishida, J. Flouquet, Review of U-based ferromagnetic superconductors: comparison between UGe_2, URhGe, and UCoGe, J. Phys. Soc. Jpn. 88 (2019) 022001, https://doi.org/10.7566/JPSJ.88.022001
[9] M. Pasturel, A. Pikul, G. Chajewski, Noël, D. Kaczorowski, Ferromagnetic ordering in the novel ternary uranium germanide $URu_{0.29}$ Ge_2, Intermetallics 95 (2018) 19, https://doi.org/10.1016/j.intermet.2018.01.011
[10] M. Pasturel, M. Szlawska, J. Ćwik, D. Kaczorowski, A. Pikul, Antiferromagnetic ordering in the ternary uranium germanide uni_{1-x} ge_2: neutron diffraction and physical properties studies, Intermetallics 131 (2021) 107112, https://doi.org/10.1016/j.intermet.2021.107112
[11] M. Henriques, D. Berthebaud, A. Lignie, Z. ElSayah, C. Moussa, O. Tougait, L. Havela, A. Gonçalves, Isothermal section of the ternary phase diagram U-Fe-Ge at 900 °C and its new intermetallic phases, J. Alloys Compd. 639 (2015) 224, https://doi.org/10.1016/j.jallcom.2015.03.145
[12] J. Rodríguez-Carvajal, Recent advances in magnetic structure determination by neutron powder diffraction, Phys. B Condens. Matter 192 (1993) 55, https://doi.org/10.1016/0921-4526(93)90108-I
[13] Y. Ōnuki, I. Ukon, S. Won Yun, I. Umehara, K. Satoh, T. Fukuhara, H. Sato, S. Takayanagi, M. Shikama, A. Ochiai, Magnetic and electrical properties of U-Ge intermetallic compounds, J. Phys. Soc. Jpn. 61 (1992) 293, https://doi.org/10.1143/JPSJ.61.293
[14] P. Boulet, M. Potel, G. André, P. Rogl, H. Noël, Crystal and magnetic structure of the binary uranium germanide U_3 Ge_5, J. Alloys Compd. 283 (1999) 41, https://doi.org/10.1016/S0925-8388(98)00873-1
[15] D. Berthebaud, O. Tougait, M. Potel, E. Lopes, J. Waerenborgh, A. Gonçalves, H. Noël, Crystal structure and electronic properties of the new compound U_3 Fe_4 Ge_4, J. Alloys Compd. 554 (2013) 408, https://doi.org/10.1016/j.jallcom.2012.11.162
[16] M. Henriques, D. Berthebaud, J. Waerenborgh, E. Lopes, M. Pasturel, O. Tougait, A. Gonçalves, A novel ternary uranium-based intermetallic U_{34} Fe_{4-x} Ge_{33}: structure and physical properties, J. Alloys Compd. 606 (2014) 154, https://doi.org/10.1016/j.jallcom.2014.03.189

[17] M.S. Henriques, D.I. Gorbunov, J.C. Waerenborgh, M. Pasturel, A.V. Andreev, M. Dušek, Y. Skourski, L. Havela, A.P. Gonçalves, Synthesis and structural/physical properties of U_3 Fe_2 Ge_7: a single-crystal study, Inorg. Chem. 54 (2015) 9646, https://doi.org/10.1021/acs.inorgchem.5b01736
[18] M. van Maaren, H. van Daal, K. Buschow, C. Schinkel, High electronic specific heat of some cubic ux3 intermetallic compounds, Solid State Commun. 14 (1974) 145, https://doi.org/10.1016/0038-1098(74)90203-8
[19] M. Henriques, D. Berthebaud, L. Pereira, E. Lopes, M. Branco, H. Noël, O. Tougait, E. Šantavá, L. Havela, P. Carvalho, A. Gonçalves, Structural and physical properties of the U_9 Fe_7 Ge_{24} uranium germanide, Intermetallics 19 (2011) 841, https://doi.org/10.1016/j.intermet.2010.12.004
[20] A. Szytuła, S. Siek, J. Leciejewicz, A. Zygmunt, Z. Ban, Neutron diffraction study of UT_2 X_2 (T=Mn, Fe, X=Si, Ge) intermetallic systems, J. Phys. Chem. Solids 49 (1988) 1113, https://doi.org/10.1016/0022-3697(88)90162-X
[21] A. Dirkmaat, T. Endstra, E. Knetsch, A. Menovsky, G. Niewenhuys, J. Mydosh, Magnetic and transport properties of various UT_2 Ge_2 (T=3d element) intermetallic compounds, J. Magn. Magn. Mater. 84 (1990) 143, https://doi.org/10.1016/0304-8853(90)90176-Q
[22] J.A. Mydosh, Spin Glasses: An Experimental Introduction, Taylor & Francis,, London, 1993.
[23] M. Szlawska, Spin-glass freezing in single-crystalline Pr_2 $NiSi_3$, Intermetallics 115 (2019) 106616, https://doi.org/10.1016/j.intermet.2019.106616
[24] S. Süllow, G.J. Nieuwenhuys, A.A. Menovsky, J.A. Mydosh, S.A.M. Mentink, T.E. Mason, W.J.L. Buyers, Spin glass behavior in URh_2 Ge_2, Phys. Rev. Lett. 78 (1997) 354, https://doi.org/10.1103/PhysRevLett.78.354
[25] D. Li, X. Zhao, S. Nimori, Ferromagnetic ordering and weak spin-glass-like effect in Pr_2 $CuSi_3$ and Nd_2 $CuSi_3$, J. Phys. Condens. Matter 21 (2009) 026006, https://doi.org/10.1088/0953-8984/21/2/026006
[26] D.X. Li, A. Dönni, Y. Kimura, Y. Shiokawa, Y. Homma, Y. Haga, E. Yamamoto, T. Honma, Y. Ōnuki, Spin-glass behaviour with extended short-range ferromagnetic order in U_2 $RhSi_3$, J. Phys. Condens. Matter 11 (1999) 8263, https://doi.org/10.1088/0953-8984/11/42/307
[27] D.X. Li, S. Nimori, Y. Shiokawa, Y. Haga, E. Yamamoto, Y. Ōnuki, Ferromagnetic cluster glass behavior in U_2 $IrSi_3$, Phys. Rev. B 68 (2003) 172405, https://doi.org/10.1103/PhysRevB.68.172405
[28] M. Szlawska, M. Majewicz, D. Kaczorowski, Ferromagnetic spin-glass behaviour in single-crystalline U_2 $IrSi_3$, J. Phys. Condens. Matter 26 (2014) 126002, https://doi.org/10.1088/0953-8984/26/12/126002
[29] M. Szlawska, D. Gnida, D. Kaczorowski, Magnetic and electrical transport behavior in the crystallographically disordered compound U_2 $CoSi_3$, Phys. Rev. B 84 (2011) 134410, https://doi.org/10.1103/PhysRevB.84.134410
[30] K. Gschneidner, J. Tang, S. Dhar, A. Goldman, False heavy fermions, Phys. B Condens. Matter 163 (1990) 507, https://doi.org/10.1016/0921-4526(90)90254-R
[31] R. Troć, Z. Gajek, A. Pikul, Dualism of the 5*f* electrons of the ferromagnetic superconductor UGe_2 as seen in magnetic, transport, and specific-heat data, Phys. Rev. B 86 (2012) 224403, https://doi.org/10.1103/PhysRevB.86.224403
[32] D. Gnida, M. Szlawska, P. Wiśniewski, D. Kaczorowski, Quantum interference in disordered ferromagnet U_2 $NiSi_3$, Acta Phys. Pol. A 127 (2015) 451, https://doi.org/10.12693/APhysPolA.127.451